Electronic Supplementary Material (ESI) for Journal of Materials Chemistry C.

A Freezing-Tolerant Superior Proton Conductive Hydrogel Comprised of Sulfonated Poly(ether-ether-ketone) and Poly(vinyl-alcohol) as Quasi-Solid-State Electrolyte in Proton Battery

Hao Dong,[a] Lin-Lin Wang,[a] Zhi-Rong Feng,[a] Jie Song,[b] Qiao Qiao,*[a,b] Yu-Ping Wu,[b] and Xiao-Ming Ren*[a,c]

[a] College of Chemistry and Molecular Engineering, Nanjing Tech University, Nanjing 211816, P. R. China

[b] School of Energy Science and Engineering, Nanjing Tech University, Nanjing 211816, P. R. China

[c] State Key Laboratory of Coordination Chemistry, Nanjing University, Nanjing 210023, P. R. China

Table of Contents

Section 1

Synthesis of nickel ferrocyanide (Ni-PBA) and molybdenum (VI) oxide (MoO_3)

The synthesis of Ni-PBA was based on a co-precipitation reaction in an aqueous solution.[1] In a typical procedure, 3 mmol $K_4Fe(CN)_6 \cdot 3H_2O$ and 0.16 mol KCl were dissolved in 150 mL deionized water under stirring to obtain a solution A. The green $NiCl_2$ solution (150 mL 0.04 mol L^{-1}) was added dropwise into solution A under vigorously stirring at 70°C. After 6 hours of reaction, the gray-green precipitates were washed and centrifuged with deionized water and ethanol for multiple times and then vacuum-dried overnight at 60 ℃.

α-MoO_3 was synthesized via a modified hydrothermal method.[2] Typically, 1.0 g $(NH_4)_6Mo_7O_{24} \cdot 4H_2O$ was dissolved in 30 mL DI water, then 10 mL HNO_3 solution (3 M) was added to adjust the pH. After stirring for 20 min, the transparent colorless solution was transferred into a Teflon-lined autoclave and heated at 180 ℃ for 24 hours. The white precipitate was obtained by centrifugation and washed with DI water and ethanol for several times, and then vacuum-dried overnight at 60 ℃.

Section 2

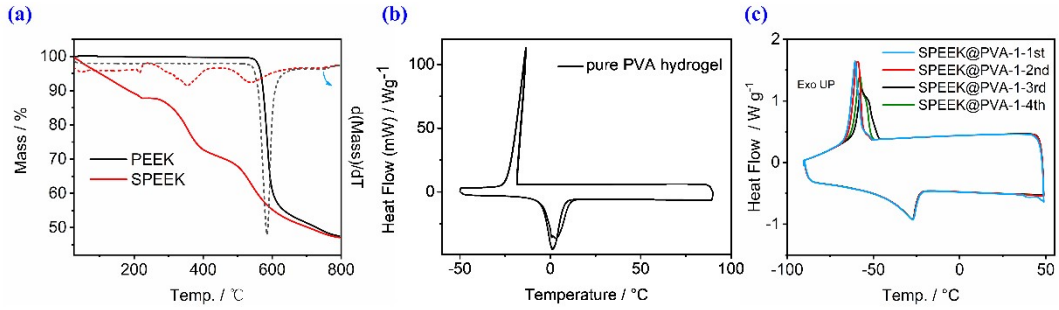

Figure S1. (a) TG plots and their first derivative curves of PEEK and SPEEK, DSC curves of (b) pure PVA hydrogel and (c) SPEEK@PVA-1 hydrogel.

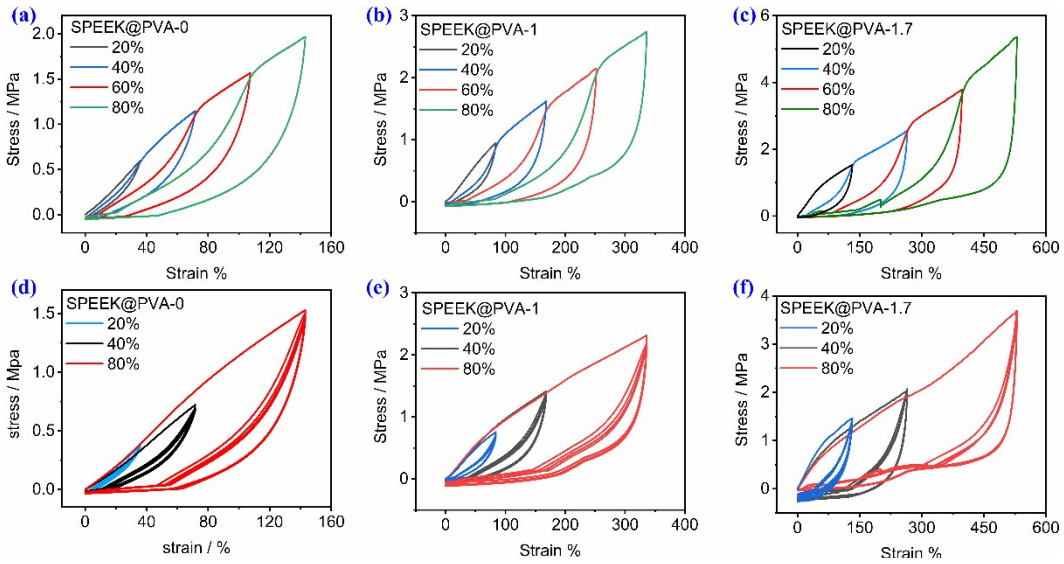

Figure S2. Successive tensile loading–unloading curves which were done sequentially at 20%, 40%, 60% and 80% of maximum strain at room temperature for SPEEK@PVA-X hydrogels (a) X = 0, (b) X = 1 and (c) X = 1.7. Tensile loading–unloading curves at 20%, 40% and 80% of maximum strain at room temperature for SPEEK@PVA-X hydrogels (d) X = 0, (e) X = 1 and (f) X = 1.7, and five successive cyclic processes of tensile loading–unloading were performed at each strain.

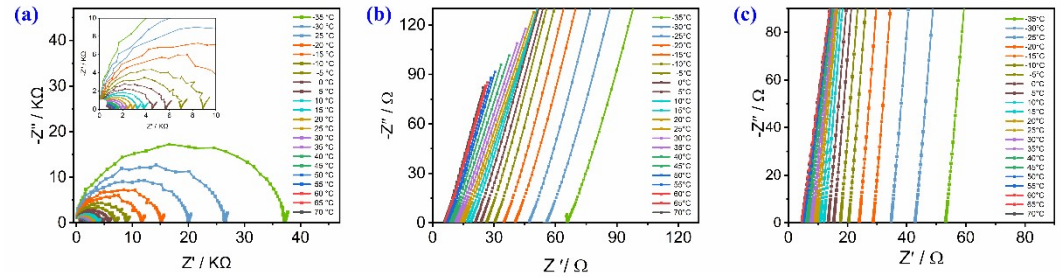

Figure S3. Temperature-dependent Nyquist plots of SPEEK@PVA-X hydrogels. (a) X = 0, (b) X = 1and (c) X = 1.7.

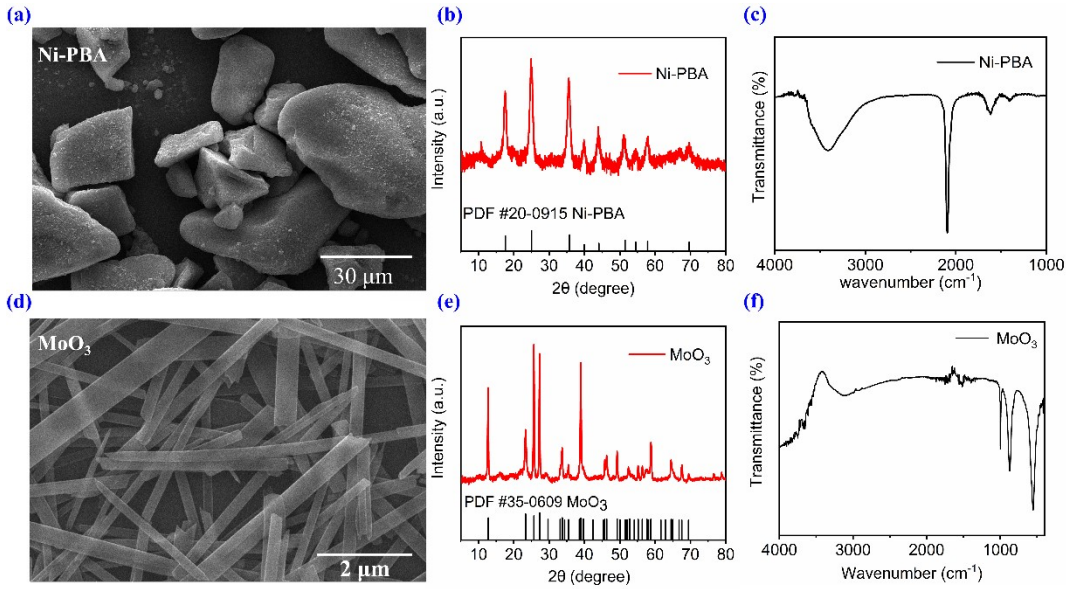

Figure S4. SEM images (a, d), PXRD patterns (b, e) and FT-IR spectra (c, f) for Ni-PBA and MoO_3. Ni-PBA was prepared by a precipitation reaction in an aqueous solution, the intense diffraction peaks in PXRD pattern of Ni-PBA, appeared in the 2θ range of 5–50°, correspond to the (2 0 0), (2 2 0), (4 0 0), (4 4 0) and (6 2 0) crystallographic plane reflections, and are good consistent with the standard PXRD card (JCPDS no. 20-0915). The intense band at 2088 cm^{-1} in FT-IR spectrum is the characteristic band of ν(C≡N) related to cyanide-coordinated Fe^{2+}, the vibration band at 3375 cm^{-1} arises from H–O stretching of interstitial water in Ni-PBA. The MoO_3 was synthesized via a modified hydrothermal method, the as-prepared nanobelt MoO_3 has a stable layered orthorhombic structure according to PXRD card (JCPDS no. 35-0609). The band at 996 cm^{-1} in FT-IR spectrum of nanobelt MoO_3 was associated with the terminal ν(Mo = O), which was an indication of layered MoO_3 phase. The bands at 867 cm^{-1} and 558 cm^{-1} are assigned to the Mo^{6+} stretching vibrations and bending vibrations of the Mo-O-Mo units.

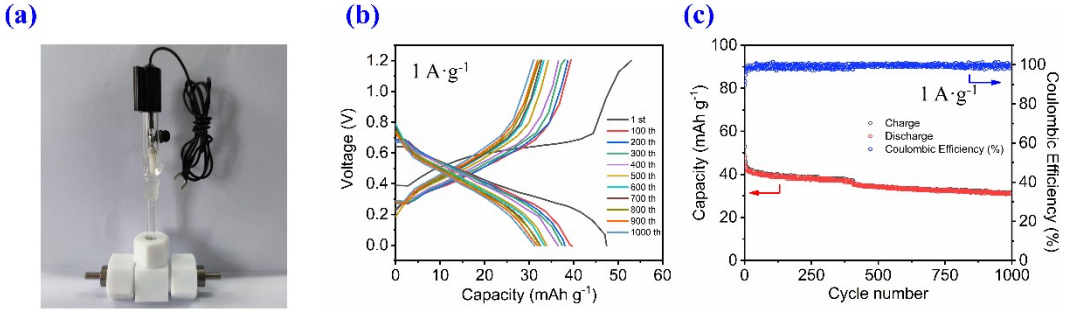

Figure S5. Electrochemical performance of proton battery with Ni-PBA and Pt electrode and SPEEK@PVA-1.7 hydrogel electrolyte. (a) Photograph of Swagelok cell (b) GCD curves and (c) Cycling and coulombic performance at a current of 1 A g^{-1} during 1000 cycles.

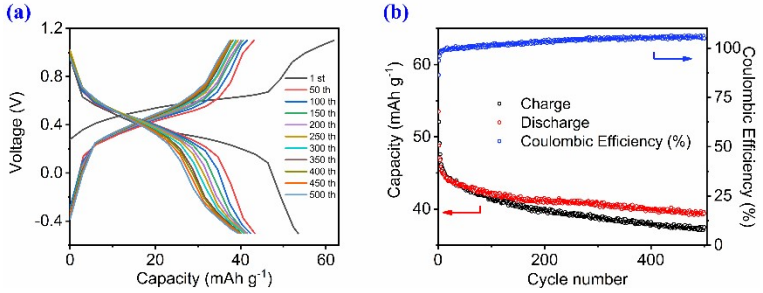

Figure S6. Electrochemical performance of full proton battery with 1 M H_2SO_4 electrolyte. (a) GCD curves and (b) Cycling and coulombic performance at a current of 1 A g^{-1} during 500 cycles.

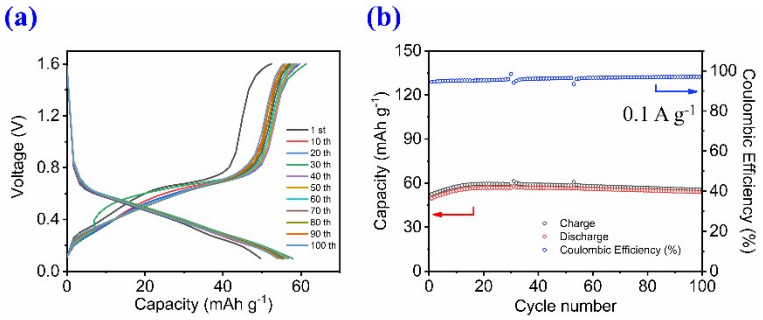

Figure S7. Electrochemical performance of full proton battery with SPEEK@PVA-1.7 hydrogel electrolyte under −20 ℃. (a) GCD curves and (b) Cycling and coulombic performance at a current of 0.1 A g^{-1} during 100 cycles.

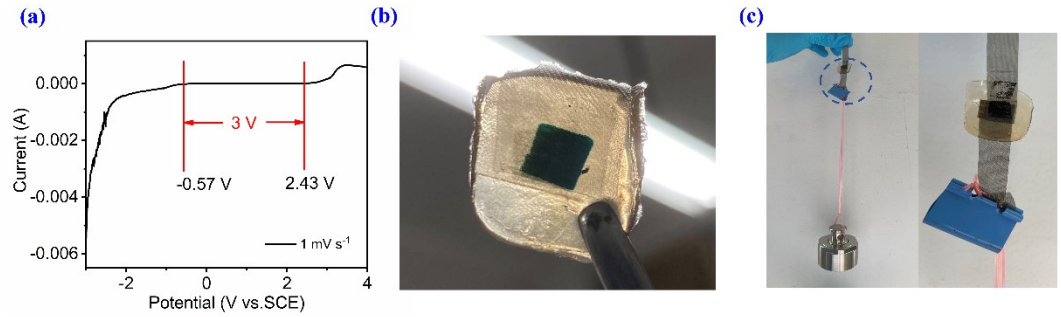

Figure S8. (a) LSV curves of SPEEK@PVA-1.7 hydrogel at the scan rate of 1 mV s^{-1}. (b) Photograph of SPEEK@PVA-1.7 hydrogel after charging-discharging 500 cycles at a current of 1 A g^{-1}. (c) Photograph of super-adhesive properties of the electrode-hydrogel interface (load weight is 425 g).

Table S1. The position of the absorption peak of each group in PEEK, SPEEK, and the corresponding vibration mode of the infrared spectrum .[3-5]

	Wavenumber / cm^{-1}	Group	Mode of vibration
PEEK	1646	C=O	ν
	1487	C-C	ν
SPEEK	1642	C=O	ν
	1501	C-C	ν
	1468	C-C	ν
	1250	O=S=O	ν_{as}
	1075	O=S=O	ν_{s}
	708	S-O	ν

Table S2.^{1}H NMR spectrum of chemical shifts and integral areas of H at different positions.[5,6]

chemical shift (ppm)	H position	Integral area
7.00-7.07	4, 6	2.00
7.07-7.15	13'	1.17
7.15-7.20	15, 19	2.10
7.20-7.26	12'	1.09
7.26-7.30	9, 10, 12, 13	0.24
7.49-7.54	10'	1
7.77-7.80	16, 18	2.09
7.80-7.88	3, 7	2.28

Table S3. The elemental analysis results of PEEK and SPEEK

Sample	N (%)	C (%)	H (%)	S (%)	S / C*
PEEK	0.00	77.86	4.102	0.000	/
SPEEK	0.00	55.15	3.704	7.121	0.129

*The sulfonated degree (n) is obtained by calculating the element ratio of C and S from the equation S / C=32n / (12 × 19), where the molar masses of C, S are 12 g/mol and 32 g/mol, respectively.

Table S4. Proton conduction of SPEEK@PVA-1.7 in comparison with other high-performing SPEEK-based proton conductors

SPEEK-based proton conductor	conductivity (mS cm^{-1})	conditions	Ref
C-SPEEK/HPW/GO	119.04	80℃	7
SiW_9MoV_2/rGO/SPEEK	10.7	16°C and 70% RH	8
SPEEK/CrPSSA 40 sIPN	1	80℃ and 25%RH	9
SPEEK/SRGO-1.0	8.6	80°C and 50% RH	10
SPEEK/ZCN-2.5	50.24	120℃ and 30%RH	11
SPEEK/P@MWCNT	64	25℃ and 100%RH	12
SPEEK/HMN-6	70	25℃ and 100%RH	13
SPEEK/P–C_3N_4	0.91	20°C and 45%RH	14
SPEEK/CeO_2-$ATiO_2$	17.06	60°C and 20%RH	15
SPEEK@PVA-1.7	51.49	25℃	**This work**
	101.2	70℃	**This work**

Table S5. A comparison of the Ni-PBA/SPEEK@PVA-1.7/MoO_3 cell with the representative proton batteries, in terms of energy density and cycling stability

Cathode Anode	Electrolyte (state)	Energy density *	Cycling stability	Ref
CuFe-TBA MoO_3	9.5 M H_3PO_4 (Liquid)	49 mAh g^{-1} and 44 mAh g^{-1} (0.025 A g^{-1} and 5 A g^{-1})	85% after 1000 cycles at 2 A g^{-1}	2
Ni-PBA MoO_3	1 M HCl+20 M $ZnCl_2$ (Liquid)	62 mAh g^{-1} and 38 mAh g^{-1} (0.5 A g^{-1} and 1A g^{-1})	76.1% after 400 cycles at 1A g^{-1}	16
In-HCF DPPZ	0.05 M H_2SO_4 (Liquid)	39.7 mAh g^{-1} (1 A g^{-1})	76.1% after 3000 cycles at 6A g^{-1}	17
PB $Ti_3C_2T_x$ MXene	1 M KNO_3+10 mM HNO_3 (Liquid)	45 mAh g^{-1} and 21 mAh g^{-1} (0.7 A g^{-1} and 6.8 A g^{-1})	74% after 3000 cycles at 6.8 A g^{-1}	18
CuFe-TBA WO_3	2 M H_2SO_4 (Liquid)	50 mAh g^{-1} (0.6 A g^{-1})	74% after 1000 cycles	19
CuFe-TBA MoO_3	1 M H_3PO_4 in MeCN (Liquid)	48 mAh g^{-1} (0.1 A g^{-1})	48% after 100 cycles	20
ZnFe-TBA MoO_3	1 M H_3PO_4 in MeCN (Liquid)	48 mAh g^{-1} (0.1 A g^{-1})	83% after 80 cycles	20
CuFe-TBA MoO_3	$[Zn_3(H_2PO_4)_6(H_2O)_3]$(1,2, 3- benzotriazole) glass (Solid)	55 mAh g^{-1} and 12 mAh g^{-1} (0.01 A g^{-1} and 0.05 A g^{-1})	-	21
Ni-PBA **MoO_3**	**SPEEK@PVA Hydrogel** **(Quasi-solid)**	**66.2 mAh g^{-1} and 49.6 mAh g^{-1}** **(0.1 A g^{-1} and 1 A g^{-1})**	**77% after 500 cycles at 1 A g^{-1}**	**This work**

*Energy density was based on the mass of the limiting electrode.

References

(1) Y. Yuan, D. Bin, X. Dong, Y. Wang, C. Wang and Y. Xia, *ACS Sustainable Chem. Eng.,* 2020, **8**, 3655-3663.

(2) H. Jiang, W. Shin, L. Ma, J. J. Hong, Z. Wei, Y. Liu, S. Zhang, X. Wu, Y. Xu, Q. Guo, M. A. Subramanian, W. F. Stickle, T. Wu, J. Lu and X. Ji, *Adv. Energy Mater.,* 2020, **10**, 2000968.

(3) W. Dai, Y. Shen, Z. Li, L. Yu, J. Xi and X. Qiu, *J. Mater. Chem. A,* 2014, **2**, 12423-12432.

(4) Q. Xin, Z. Li, C. Li, S. Wang, Z. Jiang, H. Wu, Y. Zhang, J. Yang and X. Cao, *J. Mater. Chem. A,* 2015, **3**, 6629-6641.

(5) P. Xing, G. P. Robertson, M. D. Guiver, S. D. Mikhailenko, K. Wang and S. Kaliaguine, *J. Membr. Sci.,* 2004, **229**, 95-106.

(6) S. M. J. Zaidi, S. D. Mikhailenko, G. P. Robertson, M. D. Guiver and S. Kaliaguine, *J. Membr. Sci.,* 2000, **173**, 17-34.

(7) F. Sun, L. L. Qin, J. Zhou, Y. K. Wang, J. Q. Rong, Y. J. Chen, S. Ayaz, Y. U. Hai-Yin and L. Liu, *J. Membr. Sci.,* 2020, **611**, 118381.

(8) H. Wu, H. Cai, Y. Xu, Q. Wu and W. Yan, *Mater. Chem. Phys.,* 2018, **215**, 163-167.

(9) X. Wu, G. He, X. Li, F. Nie, X. Yan, L. Yu and J. Benziger, *J. Power Sources,* 2014, **246**, 482-490.

(10) X. Qiu, T. Dong, M. Ueda, X. Zhang and L. Wang, *J. Membr. Sci.,* 2017, **524**, 663-672.

(11) H. Sun, B. Tang and P. Wu, *ACS Appl. Mater. Interfaces,* 2017, **9**, 35075-35085.

(12) Z. Esmaeilzadeh, M. Karimi, A. M. Shoushtari and M. Javanbakht, *Polymer,* 2021, **230**, 124067.

(13) S. Zhai, Z. Lu, Y. Ai, X. Liu, Q. Wang, J. Lin, S. He, M. Tian and L. Chen, *J. Membr. Sci.,* 2022, **645**, 120214.

(14) S. Zhai, H. Song, X. Jia, K. Yang, M. Feng, S. He and J. Lin, *J. Power Sources,* 2021, **506**, 230195.

(15) H. Ranganathan, M. Vinothkannan, A. R. Kim, V. Subramanian, M.-S. Oh and D. J. Yoo, *Int. J. Energy Res.,* 2022, **46**, 9041-9057.

(16) B. Yang, T. Qin, Y. Du, Y. Zhang, J. Wang, T. Chen, M. Ge, D. Bin, C. Ge and H. Lu, *Chem. Commun.,* 2022, **58**, 1550.

(17) J. Qiao, M. Qin, Y.-M. Shen, J. Cao, Z. Chen and J. Xu, *Chem. Commun.,* 2021, **57**, 4307.

(18) Y. Zhu, Y. Lei, Z. Liu, Y. Yuan and H. N. Alshareef, *Nano Energy,* 2021, **81**, 105539.

(19) X. Wu, J. J. Hong, W. Shin, L. Ma, T. Liu, X. Bi, Y. Yuan, Y. Qi, T. W. Surta, W. Huang, J. Neuefeind, T. Wu, P. A. Greaney, J. Lu and X. Ji, *Nat. Energy,* 2019, **4**, 123-130.

(20) Y. Xu, X. Wu, H. Jiang, L. Tang, K. Y. Koga, C. Fang, J. Lu and X. Ji, *Angew. Chem. Int. Ed.,* 2020, **59**, 22007-22011.

(21) N. Ma, S. Kosasang, A. Yoshida and S. Horike, *Chem. Sci.,* 2021, **12**, 5818.